Supplementary Material:

Supplementary Table 1: Gene expression profiling of 2-month-old Tfam-SCKO nerves. List of differentially expressed genes with at least 2.0 fold differential regulation between 2-month-old Tfam-SCKO and Ctrl nerves as determined by a two class unpaired SAM analysis. False discovery rate (FDR) = 0.5%.

Supplementary Figure 1: Increased mitochondrial content and glycolysis help maintain cellular energy levels following mitochondrial dysfunction in Tfam-deficient SCs. (A) qRT-PCR results showing depletion of mtDNA content and mitochondrially-encoded electron transport chain subunit transcripts (mt-ND2 and mt-Cox1) in the sciatic nerves of 2-month-old Tfam-SCKO vs. Ctrl mice. N=3-5 mice per genotype. *P<0.05. **(B)** Reduced mitochondrial COX activity (complex IV), which contains critical mtDNA-encoded subunits, as measured in mitochondria isolated from the sciatic nerves of 2-month-old Tfam-SCKOs vs. Ctrls. N=3 pools of 2 mice per genotype. *P<0.01. **(C)** Reduced mitochondrial respiration in 2-month-old Tfam-SCKO permeabilized sciatic nerves vs. Ctrls measured using high resolution respirometry. Reduced respiration was observed with substrates delivering electrons to complex I (pyruvate+malate) or to complexes I and II together (pyruvate+malate+succinate). N=5 mice per genotype. *P<0.05. **(D)** Loss of COX enzymatic staining from SCs (arrowheads) in sciatic nerves of 4-month-old Tfam-SCKOs compared to Ctrls, indicating mitochondrial dysfunction specifically in this cell type. Scale bar 25 μm **(E)** Electron micrographs of Tfam-SCKO sciatic nerves show abundant abnormal enlarged mitochondria (white arrowheads) in SCs (SC), while axonal (A) mitochondria (black arrowheads) show no morphological abnormalities. Pathological mitochondria are visible as early as 1 month of age in Tfam-SCKO nerves (left panel) and become more abundant as these mice age (4-month-old right panel). Scale bars: 500 nm. **(F)** Immunoblot analysis and quantification of band intensity (OD, optical density) of porin, a mitochondrial membrane protein that serves as a reliable marker of mitochondrial content, shows a 3-fold increase in 2-month-old Tfam-SCKO vs. Ctrl nerves. N=3 mice per genotype. *P<0.05. **(G)** Increased ratio of maximum complex IV activity per mg of tissue vs. maximum complex IV activity per mg of mitochondria for 2-month-old Tfam-SCKOs confirms a higher mitochondrial content in these mice. N= complex IV activity measured from 5 whole nerves and from 4 nerve

mitochondria preparations. *P<0.05. **(H)** Lactate levels in 2-month-old Tfam-SCKO nerves are greater than in Ctrl nerves, suggesting increased glycolysis. N=8 mice per genotype. *P<0.05.

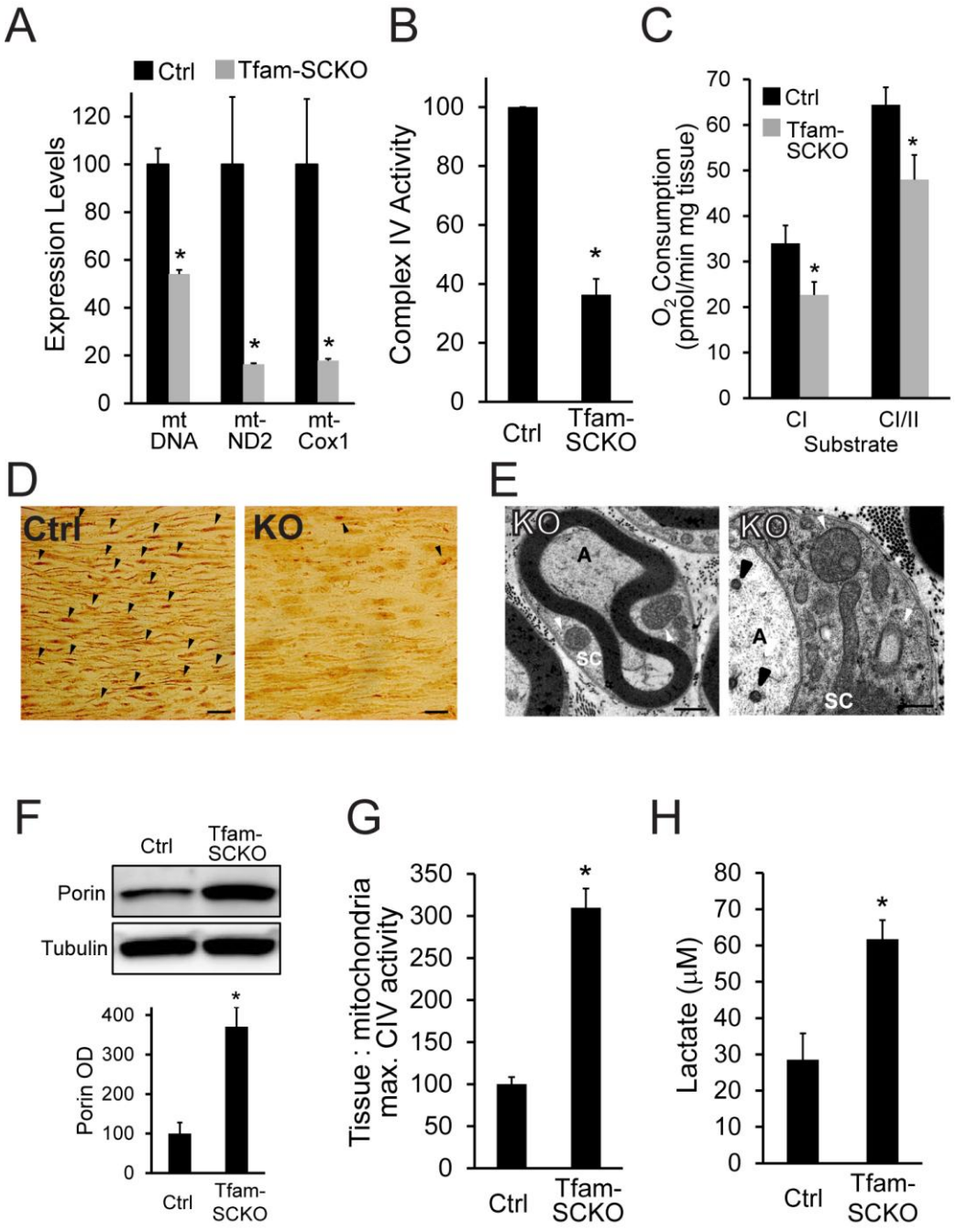

Supplementary Figure 2: Normal nodal architecture and axon-SC interactions in 1-month-old Tfam-SCKO nerves with unaltered sulfatide and cerebroside content. (A, B) Lipidomic analysis shows no significant differences in cerebrosides (A) and sulfatides (B) in 1-month-old Tfam-SCKO vs. Ctrl nerves. N=3 mice per genotype. **(C)** Immunostaining of teased nerve fibers from 3-week-old Tfam-SCKO and Ctrl mice with antibodies against nodal (Nav1.6), paranodal (Caspr) and juxtaparanodal (Kv1.1) markers confirms that nodal architecture initially develops normally in these mice and remains undisrupted for as long as sulfatide and cerebreoside nerve levels remain unchanged. Scale bar 50 μm. **(D)** Electron micrographs from 3-week-old Tfam-SCKO sciatic nerves and littermate Ctrls confirm that axon-glia interactions as well as nodes of Ranvier initially develop normally and remain undisrupted for as long as sulfatide and cerebreoside nerve levels remain unchanged. N, node; Mv, microvilli; Pn, paranode; arrowheads, paranodal loops. Scale bar 2 μm in main panels, 500 nm in magnified panels. **(E)** Quantification of the number of nodes in 1-month-old Ctrl and Tfam-SCKO nerves with intact Kv1.2 clusters (both) or with missing Kv1.2 clusters at either one (half) or both sides of the node (none). Nodal architecture was visualized by immunostaining of longitudinal nerve sections with antibodies against Caspr and Kv1.2 and no significant differences were detected at this age. N=3 mice per genotype.

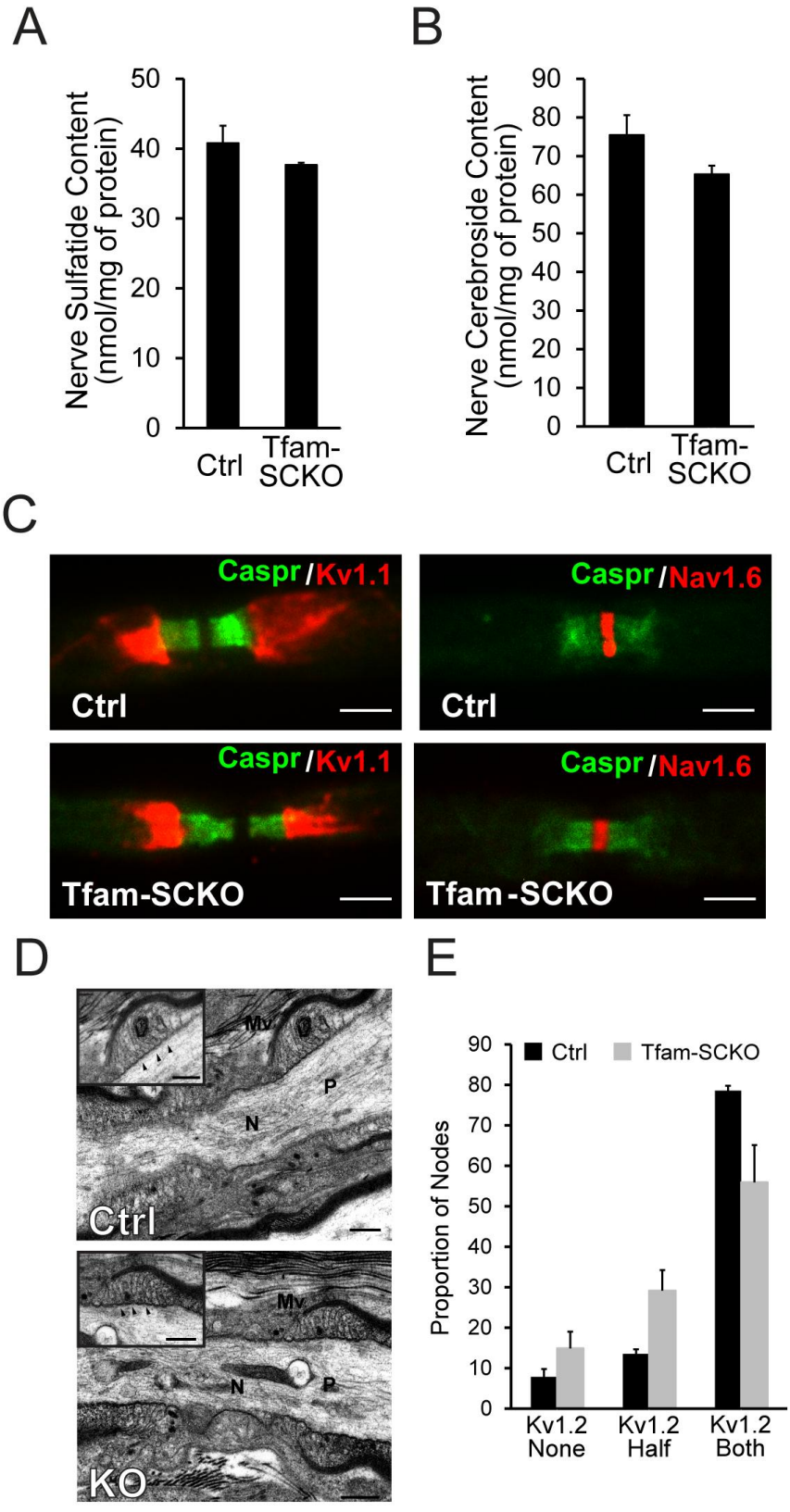
A
Nerve Sulfatide Content (nmol/mg of protein)
50
40
30
20
10
0
Ctrl
Tfam-SCKO
B
Nerve Cerebroside Content (nmol/mg of protein)
90
80
70
60
50
40
30
20
10
0
Ctrl
Tfam-SCKO
C
Caspr/Kv1.1
Ctrl
Caspr/Nav1.6
Ctrl
Caspr/Kv1.1
Tfam-SCKO
Caspr/Nav1.6
Tfam-SCKO
D
Mv
P
N
Ctrl
Mv
N
P
KO
E
Ctrl
Tfam-SCKO
Proportion of Nodes
90
80
70
60
50
40
30
20
10
0
Kv1.2 None
Kv1.2 Half
Kv1.2 Both

Supplementary Figure 3: Early and severe accumulation of acylcarnitine fatty acid β-oxidation intermediates in Tfam-SCKO nerves. (A, B) Lipidomic analysis shows a significant accumulation of long-chain acylcarnitines (total, A) that affects most long-chain molecular species (B) in Tfam-SCKO vs. Ctrl nerves as early as 1 month of age. This is the first detectable lipid abnormality in the nerves of these mice. Error bars, SEM. n=3 mice per genotype. *P<0.05. **(C, D)** Representative spectra of acylcarnitine species detected in 2-month-old Ctrl (C) and Tfam-SCKO (D) nerves depict the peak of the dramatic accumulation of this lipid class in SCs following mitochondrial dysfunction. Asterisks mark two of the more increased acylcarnitines species m/z = 398.3, C16:1; m/z = 426.3, C18:1. IS, internal standard. **(E)** Lipidomic analysis also shows the accumulation of hydroxy-acylcarnitine species (derived from 3-hydroxy acyl CoA) in Tfam-SCKO nerves, indicative of inhibition of the β-oxidation reaction catalyzed by 3-hydroxyacyl CoA dehydrogenase. n=5 mice per genotype. *P<0.05. ***f)*** Reduced NAD+/NADH ratio in Tfam-SCKO nerves. Error bars, SEM. n=6 mice per genotype. *P<0.05.

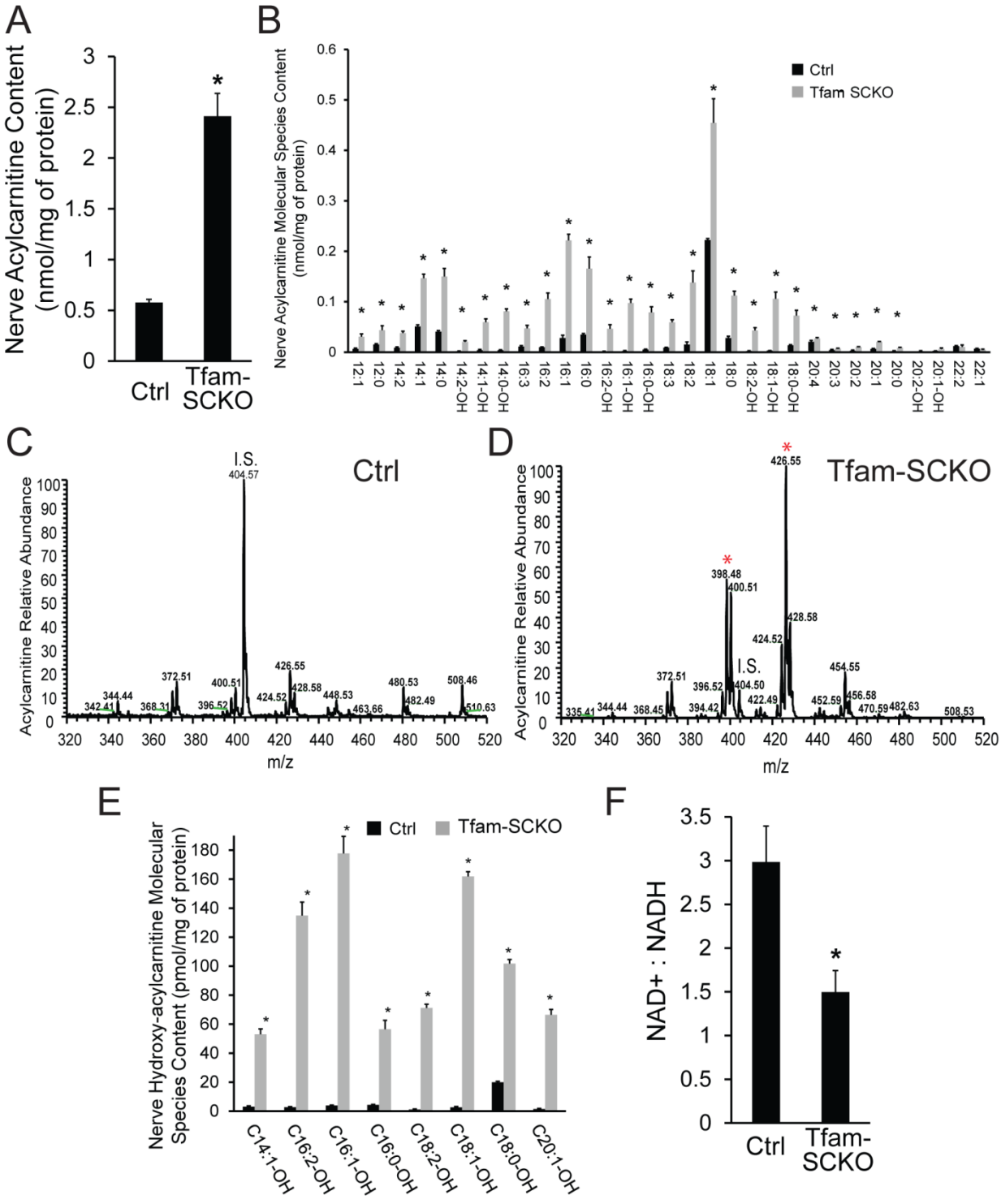
A
Nerve Acylcarnitine Content (nmol/mg of protein)
Ctrl
Tfam-SCKO
B
Nerve Acylcarnitine Molecular Species Content (nmol/mg of protein)
Ctrl
Tfam SCKO
12:1
12:0
14:2
14:1
14:0
14:2-OH
14:1-OH
14:0-OH
16:3
16:2
16:1
16:0
16:2-OH
16:1-OH
16:0-OH
18:3
18:2
18:1
18:0
18:2-OH
18:1-OH
18:0-OH
20:4
20:3
20:2
20:1
20:0
20:2-OH
20:1-OH
22:2
22:1
C
Ctrl
I.S.
404.57
Acylcarnitine Relative Abundance
m/z
D
Tfam-SCKO
426.55
398.48
400.51
428.58
424.52
I.S.
404.50
Acylcarnitine Relative Abundance
m/z
E
Ctrl
Tfam-SCKO
Nerve Hydroxy-acylcarnitine Molecular Species Content (pmol/mg of protein)
C14:1-OH
C16:2-OH
C16:1-OH
C16:0-OH
C18:2-OH
C18:1-OH
C18:0-OH
C20:1-OH
F
NAD+ : NADH
Ctrl
Tfam-SCKO

Supplementary Experimental Procedures:

Antibodies: Primary and secondary antibodies used for immunohistochemistry were as follows : Kv1.2 (1:100, rabbit, Millipore), Kv1.1 (1:100, rabbit, Abcam), Nav1.6 (1:100, rabbit, Millipore), Caspr (1:1000, mouse, gift from Dr. Elior Peles, Weizmann Institute of Science, Rehovot, Israel), goat anti-mouse Cy5 (1:250, Jackson Immunoresearch), and goat anti-rabbit Cy3 (1:500, Jackson Immunoresearch).

Primary and secondary antibodies used for Western Blots were as follows: p-AMPKα, AMPKα, p-ACC, ACC, p-Perk, p-eIF2α, and eIF2α were all raised in rabbit, used 1:1000 and purchased from Cell Signaling. We also used mouse anti-Porin (31HL, 1:1000, Calbiochem), anti-β actin (1:1000, Sigma), anti-myelin basic protein (SMI 94, 1:1000, Covance), anti-CHOP (1:1000, Cell signaling), and anti-BiP (1:1000, BD Bioscience). The secondary antibodies used were anti-mouse and anti-rabbit HRP (1:5000; Jackson ImmunoResearch Laboratories).

Primer sequences: The sequences of the qRT-PCR primers used are as follows (5'-3'; mouse unless specified): mt-ND2: F, CGCCCCATTCCACTTCTGATTACC; R, TTAAGTCCTCCTCATGCCCCTATG. mt-Cox1: F, GAACCCTCTATCTACTATTCGG; R, CAAGTCAGTTTCCAAAGCCT. SDHB: F, TGTAGAGAAGGCATCTGTGG ; R, CGTAGAAGTTACTCAAATCAGGG. mtDNA: F, AAGTCGTAACAAGGTAAGCA; R, ATATTTGTGTAGGGCTAGGG. Nuc.DNA: F, GGGTATATTTTTGATACCTTCAATGAGTTA; R, TCTGAAACAGTAGGTAGAGACCAAAGCATF4: F, GGCTATGGATGATGGCTTGG, R, AATTGGGTTCACTGTCTGAGG; ATF4 (rat): F, CTTAAGCCATGGCGCTCTTC, R, TTGCTGGTATCGAGGAATGTG ; Ddit3/Chop: F, AAGTGCATCTTCATACACCACC, R, TTGATTCTTCCTCTTCGTTTCCTG; Ddit3/Chop (rat): F, CTGAGGAGAGAGTGTTCCAG, R, GTGTGGTGGTGTATGAAGATG; ASNS: F, GCCCAAGTTCAGTATCCTCTC, R, TAAATACATGCCCACAGATGCC; mthfd2: F, AATTAAGCGAACAGGCATTCCA, R, AGGATCGTGTGCTTCTTCAG; Trib3: F, CACTTTAGCAGCGGAAGAGG, R, GTGTAGCTCGCATCTTGTCC; Trib3 (rat): F, TGTCTTCAGCAACTGTGAGAGGACGAA, R, GTAGGATGGCCGGGAGCTGAGTAT; Srebp1: F, CATGCCATGGGCAAGTACAC, R, TGTTGCCATGGAGATAGCATCT; FASN: F, GGGTGCTGACTACAACCTCTCC, R, TGCACAGACACCTTCCCGTC; HMGCR: F, TGGTGGGACCAACCTTCTAC, R,

GCCATCACAGTGCCACATAC; Acly: F, AGGAAGTGCCACCTCCAACAGT, R, CGCTCATCACAGATGCTGGTCA; ACC2: F, GGGCTCCCTGGATGACAAC, R, TCTTCCGGGAGGAGTTCT; GAPDH: F, TGCCCCCATGTTTGTGATG, R, TGTGGTCATGAGCCCTTCC. Xbp-1: F, GGCCTTGTGGTTGAGAACCAGGAG; R, GAATGCCCAAAAGGATATCAGACTC.

Nerve histology, morphometry, and immunohistochemistry: For nerve histology and morphometry, sciatic nerves from Ctrl and Tfam-SCKO mice at different ages were dissected and placed in 3% glutaraldehyde overnight. After washing with phosphate buffer, nerves were postfixed in 1% osmium tetraoxide in phosphate buffer overnight at 4°C. Specimens were then dehydrated in graded alcohols and embedded in 100% epoxy (Araldite 502). One-μm-thick plastic embedded sections were prepared and stained with toluidene blue for light microscopy. For electron microscopy, fifty- to one hundred-nm-thick ultrathin sections were prepared, stained with uranyl acetate and lead citrate, and photographed with a JEOL (Akishima) 1200 electron microscope. All nerves underwent qualitative assessment of neural architecture followed by detailed histomorphometric analysis carried out as previously described (Hunter et al., 2007).

For immunohistochemical analysis of sciatic nerves, nerves were dissected and fixed in 4% paraformaldehyde for 1 h. Nerves were cryopreserved in 30% sucrose and embedded in Tissue-Tek OCT Compound (Sakura Finetek) prior to sectioning at 6 μm. For analysis of teased nerve fibers, mouse sciatic nerves were dissected and incubated in 4% paraformaldehyde in PBS for 30 min at room temperature. The nerves were washed three times in PBS for 5 min and de-sheathed, and bundles of nerve were dissected with fine needles in PBS on Fisherbrand Superfrost/Plus microscope slides. Slides were air dried for at least 2hrs at room temperature and stored at -20°C until staining.

All frozen sections were immunostained by post-fixing in ice-cold acetone at -20°C for 10 min and blocking in 5% fish skin gelatin in PBS-0.2% Triton for 1 h at room temperature. Sections were then incubated with primary antibody (see Supplementary Experimental Procedures for details) diluted in blocking buffer overnight at 4°C. Secondary antibody incubation was performed at room temperature for 1 h also in blocking buffer. After all stainings, sections were mounted with Vectashield Mounting Medium with DAPI (Vector Laboratories) for microscopic visualization. Images were captured using an upright microscope equipped for

epifluorescence microscopy (Nikon 80i; CoolSnapES camera) and were processed using MetaMorph and Image-J. For nodal quantification, at least 50 nodes in longitudinal nerve sections from 3 different mice per genotype at each time point were assessed and quantified at a 20x magnification.

Metabolite measurements: For ATP, ADP, AMP, and lactate measurements sciatic nerves were excised from Ctrl and Tfam-SCKO mice, weighted, and metabolites extracted with 1M perchloric acid (10 to 1 volume : weight). Extracts were centrifuged and neutralized with 3 M potassium carbonate. For ATP, ADP and AMP determination, neutralized extracts were diluted 1:10 with potassium phosphate buffer and assayed by HPLC (Shimazu) using an LC-18T HPLC column (Supelco) at flow rate of 1 ml/min and the absorbance at 254 nm was recorded. Each elution peak was compared with standards for identification and quantification and levels were normalized to tissue weight. EC was defined as follows: EC=[ATP]+1/2[ADP])/([ATP]+[ADP]+[AMP]. Lactate levels were determined spectrophotometrically as previously described (Marbach and Weil, 1967). NAD+, NADH+ and the NAD+/NADH ratio was determined using a CycLex NAD+/NADH colorimetric assay kit (MBL International) according to the manufacturer's protocol.

Western Blotting: Sciatic nerves were isolated, desheathed in PBS, and immediately frozen in liquid nitrogen. Lysates were prepared by homogenizing the tissue by sonication in a buffer containing 150 mM sodium chloride, 50 mM Hepes, 1% NP-40, 1 mM EDTA, 1 mM sodium fluoride, 1mM sodium orthovanodate, and complete protease inhibitor cocktail (Roche Applied Science). The lysates were clarified by centrifugation at 14,000 rpm for 10 min and quantified using the MicroBCA Protein Assay kit (Pierce). For Western blotting, the proteins were separated by SDS-PAGE and transferred to a PVDF membrane (Millipore). Membranes were blocked in 5% milk in 0.5% TBS-Tween and incubated overnight with the appropriate primary antibody (see Supplementary Experimental Procedures for details). Following incubation with secondary antibodies conjugated to HRP (GE Healthcare), membranes were developed with SuperSignal West Dura substrate (Pierce). Optical density of the signals was determined using Image-J.

Xbp-1 splicing RT-PCR: xbp-1 splicing in Ctrl and Tfam-SCKO nerves as well as in cultured SCs was determined from cDNA in a 25 μl PCR reaction with a single 4 min 94ºC denaturation cycle followed by 35 cycles of 94ºC for 10 s, 63ºC for 30 s, and 72ºC for 30 s followed by separation of the unspliced (254 bp) and spliced (229 bp) XBP-1 RT-PCR products on a 10 cm 2% agarose gel (see Supplementary Experimental Procedures for primers). Explanted nerves maintained in 10% fetal bovine serum (FBS) supplemented with 2 mM L-glutamine and 100 ng/ml of nerve growth factor in the presence of 10 μg/ml of tunicamycin served as a positive control for nerve samples.

eIF2α kinase shRNA knockdown in 3T3 cells and in vitro ISR induction: NIH 3T3 cells were infected with lentivirus expressing shRNA to one of the four eIF2α kinases (HRI, PKR, PERK, GCN2). The infected cells were selected by growth in puromycin for 5 d. Cell populations with significant knockdown of each of the kinases (% mRNA knock-down: HRI=84.8 +/- 0.3%; PKR=74 +/- 5%; PERK=63 +/- 9%; GCN2= 88 +/- 3.8%) were obtained and frozen as 'polyclonal populations'. The shRNA constructs from the RNAi Consortium collection (Moffat et al., 2006) were acquired from the Washington University RNAi Core (targeting sequences: Control luciferase, GTTGTGTTTGTGGACGAAGTA; HRI, GCTCGGAATTGGAAGGGAATT; PKR, GCCTCTTTATTCAAATGGAAT; PERK, CCATACGATAACGGTTACTAT; GCN2, GCCTGTCGAATGAAAGTGTTA). Polyclonal populations of cells with knockdown of each of the 4 eIF2α kinases were seeded onto 24-well plates (~50,000 cells/well) in 10% FBS-DMEM media. Sixteen hr after seeding, cells were treated with either vehicle or 5 μM CCCP for 3 hrs (for p-eIF2α induction) or 6 hrs (for DDIT3/CHOP induction). Cells were then harvested for Western Blot analysis.

mtDNA content quantification: mtDNA content was quantified by qRT-PCR using a SYBR green-based detection system on a 7700 Sequence Detector instrument (Applied Biosystems) in a similar way as described previously (Nagarajan et al., 2001). Instead of cDNA, however, 15ng of total DNA were used per reaction. Primers that recognized a region unique to the mitochondrial genome were used to determine the mtDNA content relative to a serial dilutions standard curve. mtDNA content values were normalized to nuclear DNA content as determined by a set of primers directed to the genomic locus of Smrt1.

Mitochondrial isolation, respiratory enzyme activity measurements, and respirometry: For mitochondrial isolation, 4 sciatic nerves were dissected, desheathed, mechanically dissociated, digested with collagenase for 20 min and pooled together in 2 ml of homogenization buffer (HM) containing 0.22 M mannitol, 70 mM sucrose, 10 mM Tris-HCl, 0.5 mM EDTA, 1mM EGTA and 0.5% delipidated BSA. Nerves were homogenized for about 2 minutes (12 strokes) using a Teflon-glass homogenizer turning at 200 rpm. The homogenate was then centrifuged at 800xg for 10 min. The clarified supernatant was centrifuged at 8,000xg for 10 min and the pellet was resuspended in 1ml of HM buffer without BSA and spun once more at 7,500xg. The resulting pellet was resuspended in 250 μl of HM buffer without BSA. The protein concentration of the resuspended mitochondrial fractions was determined using a MicroBCAProtein Assay kit (Pierce). Five micrograms of protein from these mitochondrial preps were used to measure complex IV activity spectrophotometrically as previously described (Birch-Machin and Turnbull, 2001). For high resolution respirometry 2 sciatic nerves were dissected, briefly digested with collagenase for 10 min, then desheathed and fluffed using a pair of fine forceps. At this point, nerve respiration was measured in a 2-ml chamber using and OROBOROS Oxygraph 2k (Oroboros) as previously described (Mancuso et al., 2010).

Nerve Cytochrome oxidase staining: Sciatic nerves were dissected fresh, placed in Tissue-Tek OCT Compound, and immediately frozen in isopentane cooled in liquid nitrogen. Tissue was then sectioned at 6 μm. Sections were placed in an incubating solution containing sucrose (100mg/ml), 3,3'-diaminobenzidine tetrahydrochloride 2 (DAB, 0.6 mg/ml), sodium phosphate buffer (final concentration 0.05 M), catalase 3 (2.6 μg/ml), and cytochrome c (1.6 mg/ml) for 60 minutes at room temperature. After incubation, sections were washed 3 times with deionized water, dehydrated in a series of ascending alcohols and cleared with xylene, and mounted using permount.

Microarray and computational analysis: total RNA samples were prepared by isolating and pooling RNA from at least 3 different 2 month old Tfam-SCKO and Ctrl mice. Replicates were prepared entirely independently from two separate pools of at least three animals each, 2 replicates were used. Total RNA concentration and purity was obtained from an absorbance ratio

at 260 nm and 280 nm. Total RNA quality was then determined by Agilent 2100 bioanalyzer (Agilent Technologies) according to manufacturer's recommendations. RNA transcripts were amplified by T7 linear amplification messageAmp TotalPrep amplification kit (ABI-Ambion) using 400 ng of each total RNA sample. The amplified RNA samples (aRNA) were then cleaned with RNA columns and quantified on a spectrophotometer, and RNA quality was determined by Agilent 2100 bioanalyzer (Agilent Technologies). 1500 ng of each aRNA were hybridized onto Illumina Mouse WG-6 v2.0 Expression Beadchips according to manufacturer's recommendations. Arrays were scanned on an Illumina BeadArray Reader. Images were quantitated by Illumina Beadscan, v3 and the resulting data was imported into Illumina GenomeStudio software, where on-slide spot replicates were averaged and individual spot probe was reported. This signal intensity data was background subtracted and quantile normalized in Illumina genome Studio. Probes having detection p-value>0.05 in all samples were removed and a two class unpaired SAM analysis was performed. Differentially expressed genes with at least 2.0 fold differential regulation between Tfam-SCKO and Ctrl nerves at a false discovery rate (FDR) of 0.5% were selected for further analysis. Gene enrichment of metabolic pathway was examined using GeneGO (Genego Inc).

Nerve sample lipid extract preparation for mass spectrometric analysis: lipid extraction of nerve samples was performed essentially as described previously (Han et al., 2008). A protein assay on each nerve sample was performed by using BCA method with bovine albumin as standard. Lipid internal standards (approximately one for each lipid class) were added based on protein content of each nerve sample. The molecular species of internal standards (e.g., $^{13}C_4$-16:0 carnitine, N-Pentadecanoyl-psychosine (N15:0 Cerebroside), N-Hexadecanoyl-sulfatide (N16:0 sulfatide) were selected because they are either stable isotope labeled species or represent <0.1% of the endogenous cellular lipid mass as demonstrated by mass spectrometric analysis of the nerve lipid extract without addition of internal standards. A modified Bligh and Dyer procedure was used to extract lipids from each nerve sample as previously described (Han et al., 2008). Each lipid extract was reconstituted in 200 μl /mg of protein (which was the measured protein content aforementioned) in chloroform/methanol (1:1, v/v). A portion of each lipid extract (e.g., 50 uL) was treated with LiOMe to hydrolyze phospholipids followed by washing with hexane as previously described (Jiang et al., 2007). The treated lipid samples were used for the analysis of

the sphingolipidome of each nerve sample. The original and treated lipid extracts were flushed with nitrogen, capped and stored at -20°C until ESI/MS analysis, typically within one week.

Lipidomic analysis of nerve lipid extracts by multi-dimensional mass spectrometry-based shotgun lipidomics: a triple-quadrupole mass spectrometer (Thermo Fisher TSQ Quantum Ultra Plus) equipped with an automated nanospray apparatus (i.e., Nanomate HD, Advion Bioscience Ltd.) and Xcalibur system software were utilized in the study as previously described (Han et al., 2008). Briefly, each originally-prepared lipid extract was diluted to < 50 pmol/uL with chloroform/methanol/isopropanol 1:2:4 (v/v/v) prior to direct infusion through a nanospray apparatus linked to the mass spectrometer for the analyses of phospholipids, lyso-phopholipids, acyl-carnitine, non-esterified fatty acids and triacylglycerols with or without the presence of a small amount of LiOH (Han and Gross, 2005). Each LiOMe-treated lipid extract was properly diluted prior to infusion to the mass spectrometer for the analyses of sphingolipids (Jiang et al., 2007). Typically, a 2-min period and 2-5-min of signal averaging in the profile mode were employed for acquisition of each survey scan and each tandem MS scan, respectively. For tandem mass spectrometry, a collision gas pressure was set at 1.0 mTorr but the collisional energy was varied with the classes of lipids as previously described (Han and Gross, 2005). All the MS spectra and tandem MS spectra were automatically acquired by a customized sequence subroutine operated under Xcalibur software. Each individual lipid species in a lipid class was identified using multi-dimensional mass spectrometry through building block analyses (Yang et al., 2009). The identified species were quantified using a two-step approach as previously described (Yang et al., 2009).

DRG neuron culture and Fluo-4 imaging: mouse DRG neurons were isolated from E12 embryos in DMEM (Sigma), dissociated by incubation in 0.25% trypsin, and resuspended (100 µl/embryo) in complete DRG medium: neurobasal medium (Invitrogen) containing 2% B27 supplement (Invitrogen), 50 ng/ml of nerve growth factor (Harlan Laboratories), 1 µM 5-fluoro-2′-deoxyuridine (Sigma), and 1 µM uridine (Sigma). Cells were then seeded onto either 24-well or 96-well cell cultures plates coated with poly-d-lysine (Sigma) and Laminin (Invitrogen) by spotting a single 0.5 µl (96-well) or 2 µl (24-well) droplet of the concentrated cell suspension, incubating for 15 min at 37 °C to allow neurons to adhere, then adding 100 µl (96-well) or 400 ul

(24-well) of complete DRG media. All experiments were carried out 5-6 days after seeding. For calcium imaging experiments, neurons were incubated with the calcium indicator Fluo-4 AM (2 μM, Invitrogen) for 30 min at 37 °C, washed by replacing half the media twice, then incubated for another 30 min to allow complete de-esterification of intracellular AM esters. Baseline fluorescence and phase images were taken at this point. Neurons were then treated either with vehicle, palmitoyl-carnitine (Sigma), or palmitate (Sigma) at the appropriate concentrations. Phase and fluorescence images were acquired every 15 minutes for up to 6 hours using an Operetta imaging system equipped with an environmental chamber (Perkin Elmer), and automated image analysis was carried out using image J. To examine the effect of chronic acylcarnitine exposure, DRG neurons were treated daily for up to nine days with vehicle or with palmitoyl-carnitine at the appropriate concentration.

Automated analysis and quantification of images: Axon degeneration, axonal calcium accumulation, and calcium containing vacuole formation were quantified using ImageJ as follows. For axon degeneration, bright field images of axons were binarized and fragmented axons were detected using particle analyzer. The ratio of fragmented axon area against the total axon area was expressed as degeneration index. Axonal calcium accumulation was quantified from the fluorescent images of axons loaded with Fluo-4 calcium sensitive dye as described above. The fluorescent intensity of the pixels over the axon area (as determined from accompanying bright field images) were summed and then normalized by the total axon area. Palmitoyl-carnitine treated axons tend to form vacuoles containing high concentration of Ca^{2+} which are recognized as spherical structures with higher Fluo-4 intensity than surrounding axons. The total area of these vacuoles was expressed as a Fluo-4 blebbing index. This index was determined by first calculating the total Fluo-4 positive axon area. Then the area of calcium containing vacuoles was quantified using binarized Fluo-4 images threshold such that only vacuoles but not the rest of axons were recognized by a particle analyzer. The total vacuole area detected was normalized against total Fluo-4 positive area to give Fluo-4 blebbing index.

Supplementary References:

-Han, X., and Gross, R.W. (2005). Shotgun lipidomics: electrospray ionization mass spectrometric analysis and quantitation of cellular lipidomes directly from crude extracts of biological samples. Mass Spectrom Rev 24, 367–412.

-Han, X., Yang, K., and Gross, R.W. (2008). Microfluidics-based electrospray ionization enhances the intrasource separation of lipid classes and extends identification of individual molecular species through multi-dimensional mass spectrometry: development of an automated high-throughput platform. Rapid Commun Mass Spectrom 22, 2115–2124.

-Jiang, X., Cheng, H., Yang, K., Gross, R.W., and Han, X. (2007). Alkaline methanolysis of lipid extracts extends shotgun lipidomics analyses to the low-abundance regime of cellular sphingolipids. Anal Biochem 371, 135–145.

-Mancuso, D.J., Sims, H.F., Yang, K., Kiebish, M.A., Su, X., Jenkins, C.M., Guan, S., Moon, S.H., Pietka, T., Nassir, F., et al. (2010). Genetic ablation of calcium-independent phospholipase A2{gamma} prevents obesity and insulin resistance during high fat feeding by mitochondrial uncoupling and increased adipocyte fatty acid oxidation. J Biol Chem 287, 29837-50.

-Moffat, J., Grueneberg, D.A., Yang, X., Kim, S.Y., Kloepfer, A.M., Hinkle, G., Piqani, B., Eisenhaure, T.M., Luo, B., Grenier, J.K., et al. (2006). A lentiviral RNAi library for human and mouse genes applied to an arrayed viral high-content screen. Cell 124, 1283–1298.

-Nagarajan, R., Svaren, J., Le, N., Araki, T., Watson, M., and Milbrandt, J. (2001). EGR2 mutations in inherited neuropathies dominant-negatively inhibit myelin gene expression. Neuron 30, 355–368.

-Yang, K., Cheng, H., Gross, R.W., and Han, X. (2009). Automated lipid identification and quantification by multidimensional mass spectrometry-based shotgun lipidomics. Anal Chem 81, 4356–4368.